

MACHINE LEARNING FOR CU SURFACE KINETIC MONTE CARLO

INTRODUCTION

Surface diffusion is one of the important phenomena on the Cu surface, preceding vacuum arcs. Diffusion takes place over much longer time scale than atomic vibration, and thus it is difficult to model in e.g. molecular dynamics (MD). The most efficient method for capturing diffusion is kinetic Monte Carlo (KMC).

We have developed a KMC model for the Cu surface [1]. For improving the accuracy of the model, we have now added detail to the way the model differentiates between different migration events that contribute to diffusion. For accommodating the vastly expanded parameter space that this detailed description of the events requires, we have turned to machine learning.

METHODS

We have used the atomic KMC program Kimocs [1]. The KMC model is parameterized by migration energy barriers E_m , illustrated in fig. 1. The rate Γ of each migration event is calculated as

$$\Gamma = \nu \exp\left(-\frac{E_m}{k_B T}\right) \quad (1)$$

where ν is the attempt frequency (same for all events in our model, fitted to MD results), k_B is the Boltzmann constant and T is temperature.

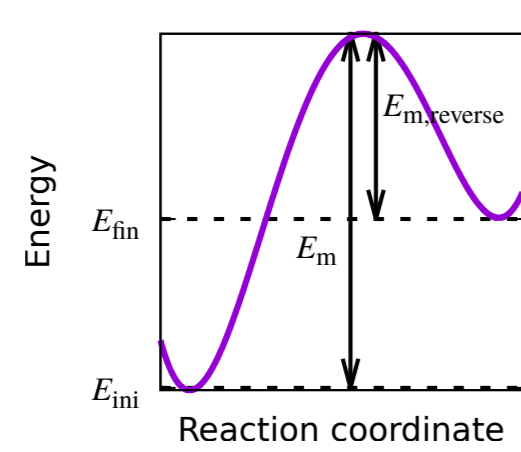


Figure 1: Schematic of the migration barrier E_m between two local potential energy minima.

The migration events are described in terms of the local atomic environment (LAE) of the migrating atom. We consider the LAE up to the second nearest neighbours of the migrating atom, comprising 26 sites in total. Thus the parameter space is 2^{26} -dimensional, with each lattice site either occupied (1) or vacant (0). This is illustrated in fig. 2.

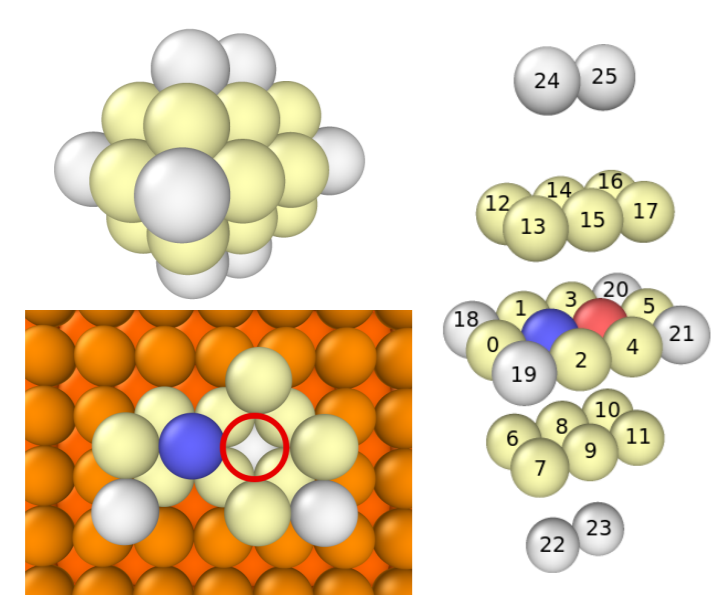


Figure 2: Our description of the local atomic environment (LAE) of the migration events. The LAE in the lower left panel would be labelled "10011111111100000001011100".

In principle [2], we can calculate the migration energy barrier of any of these 67 million cases with the nudged elastic band (NEB) method [3, 4]. The most pressing issue is the sheer amount of required NEB calculations. We overcome this obstacle by first calculating a subset of the migration barriers with NEB, and then making an artificial neural network (ANN) regression model to obtain barriers for arbitrary events on-the-fly.

We used multilayer perceptrons from the FANN library [5] for the regression task. The data set of barriers was calculated with the LAMMPS [6] implementation of the NEB method. Details of our methods will be published in ref. [7]. For assessing the success of the ANN regression we look at the error the ANN makes in the training data set, and the results of KMC simulations ran with the ANN parameterization.

RESULTS

Fig. 3 shows the correlation graph of true vs. ANN-predicted energy barriers, as well as the correlation between the true and predicted energy changes ΔE . Most of the data points are concentrated near the identity line, while the root mean square error is rather large, 0.087 eV. The significance of the error, as well as the outlier points, should become evident in the simulation tests. The good ΔE correlation gives insight on the accuracy of the thermodynamic accuracy of the model.

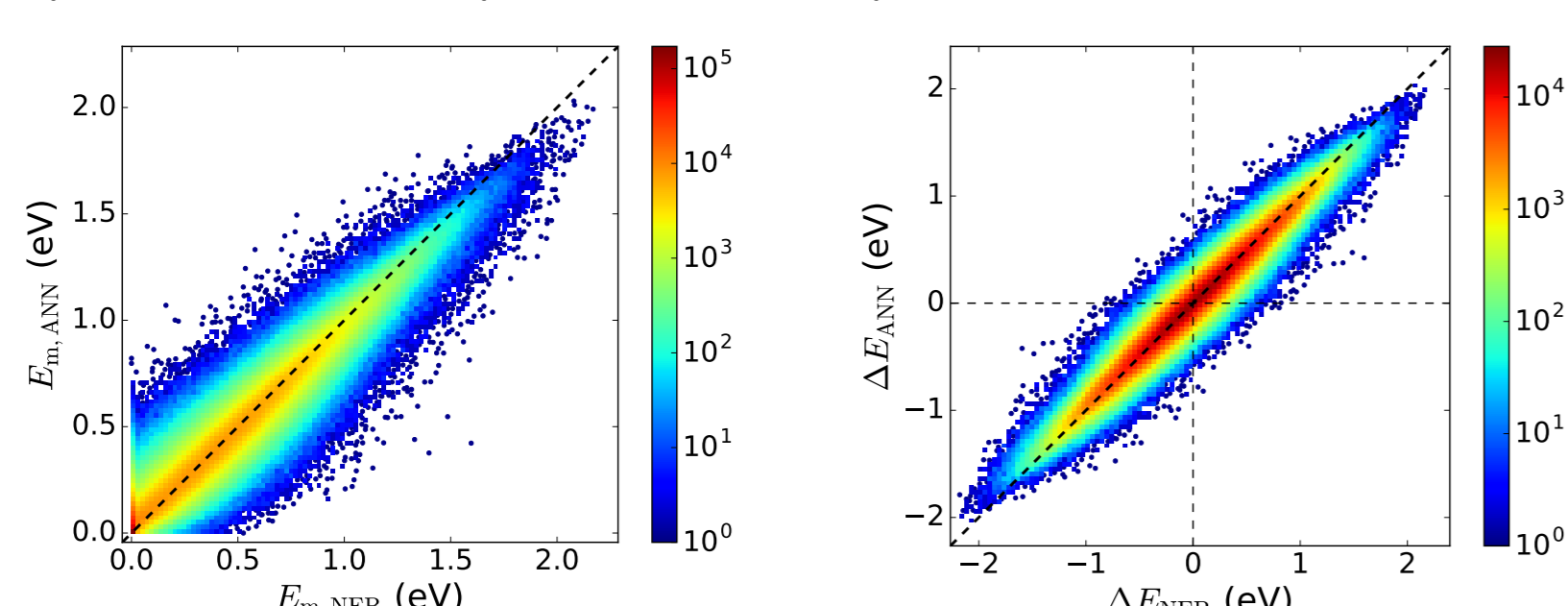


Figure 3: (left) Accuracy of the ANN regression. The root mean square error is 0.086 eV. (right) ANN prediction of the $\Delta E = E_{fm} - E_{mi}$ values. The network has learned these values only indirectly.

Fig. 4 shows initial and final configurations of cuboid nanoparticle flattening simulations on three different surface orientations. The behaviour of the systems looks quite identical to what was observed in similar experiments in ref. [1].

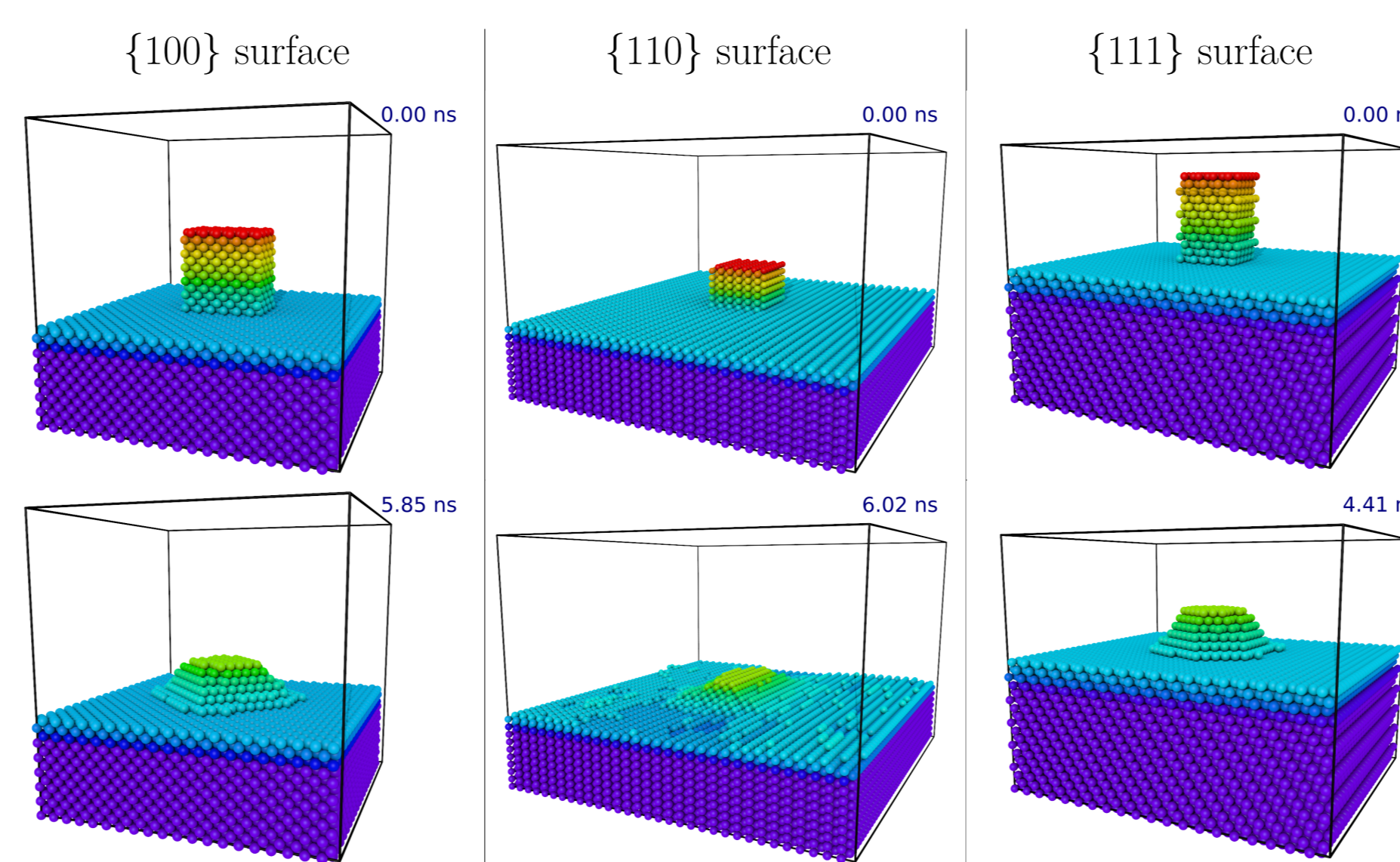


Figure 4: Flattening of a 12 monolayer, 576 atom cuboid on differently oriented surfaces. The simulations were stopped when the height of the nanoparticle reached half of the original height of 12 monolayers.

The attempt frequency ν was fitted to value $2.71 \times 10^{14} \text{ s}^{-1}$ by comparing the flattening times on the $\{110\}$ surface to corresponding MD simulations from ref. [1] at different temperatures from 850 to 1200 K. Fig. 5 shows the flattening time t_f as a function of temperature. The flattening times on all different surfaces at 1000 K are tabulated in table 1.

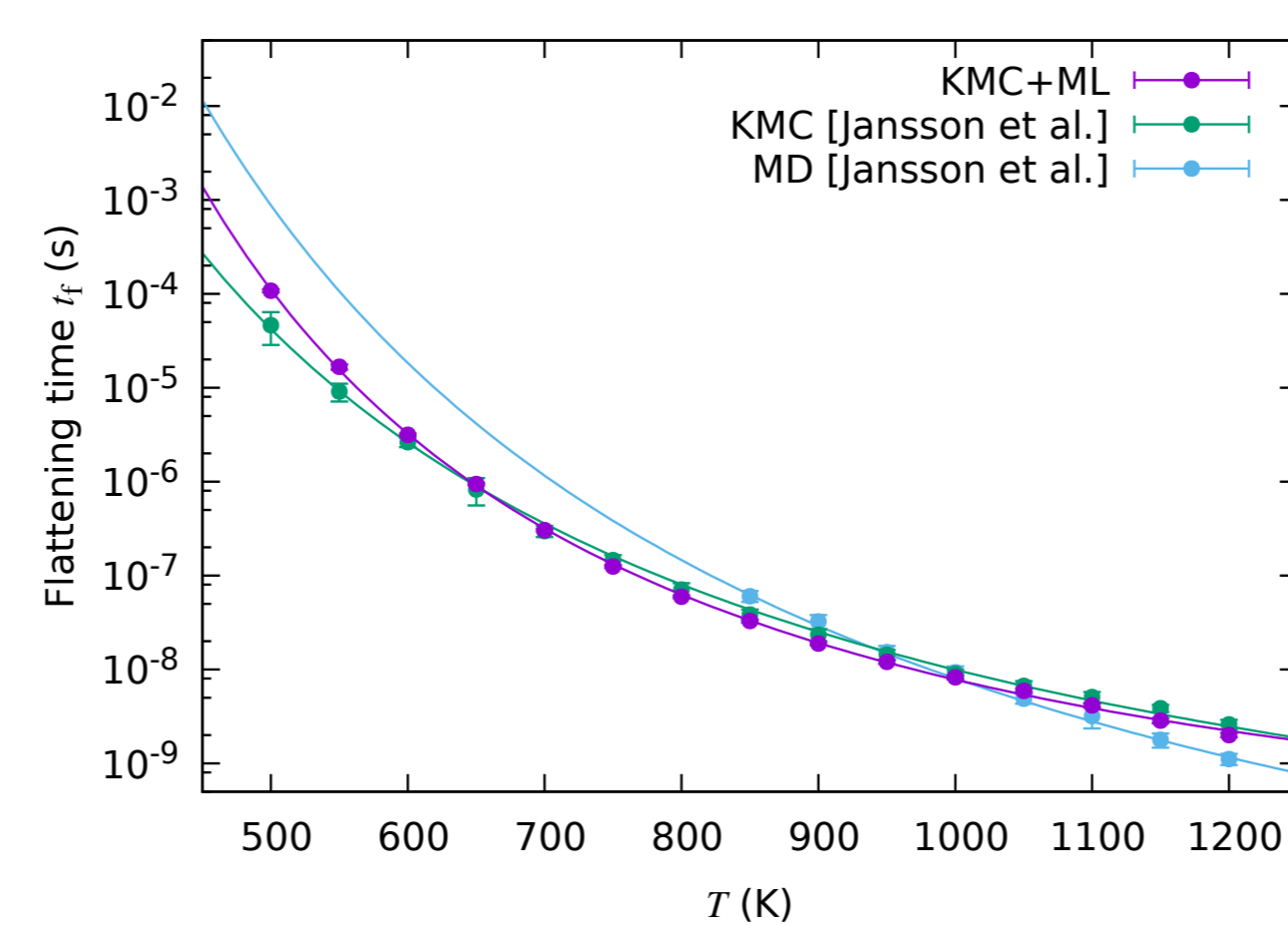


Figure 5: Flattening time of the 12 monolayer cuboid on the $\{110\}$ surface as a function of temperature. KMC+ML refers to this work. The attempt frequency was fitted for the best agreement between the MD results from ref. [1].

Table 1: Flattening time of the 12 monolayer nanoparticle at 1000 K on the different surfaces.

Surface	KMC+ML (ns)	KMC [1] (ns)	MD [1] (ns)
{100}	5.40 ± 0.13	31.0 ± 6.61	1.62 ± 0.60
{110}	6.2 ± 0.6	9.25 ± 1.10	9.29 ± 1.44
{111}	5.0 ± 0.2	18.8 ± 0.96	6.01 ± 1.48

In some cases from temperatures 950 K upwards, the $\{110\}$ surface was observed to develop large $\{100\}$ and $\{111\}$ facets before the nanoparticle had time to flatten, preventing flattening altogether. Fig. 6 shows an example of such simulation.

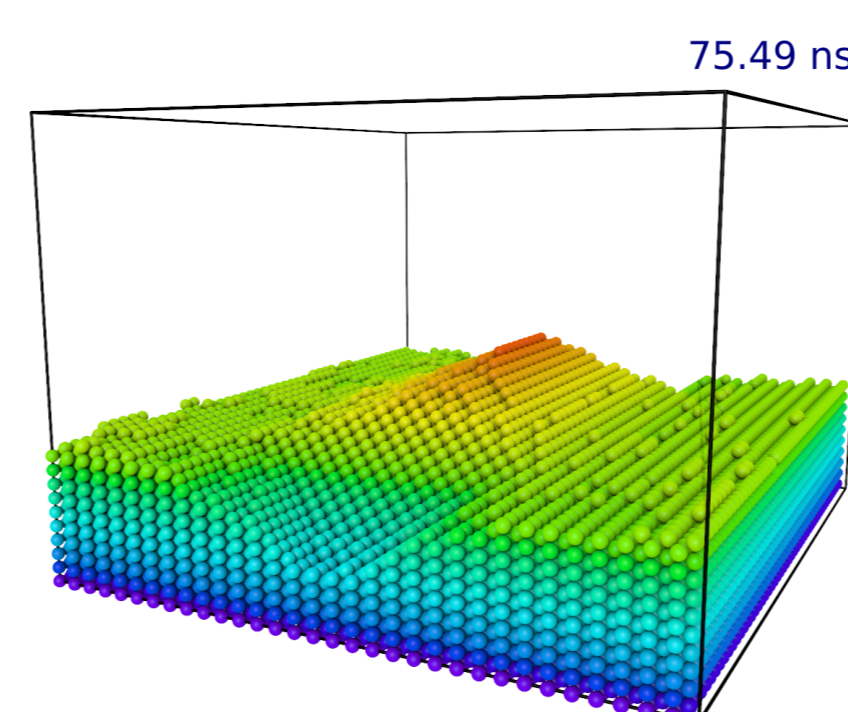


Figure 6: Snapshot of a roughened $\{110\}$ surface at 1000 K. Initially a cuboid nanoparticle was present on the surface.

The probability for the development of facets, or *roughening*, as a function of temperature, is shown in fig. 7. A roughening transition near 1000 K agrees well with earlier experimental [8, 9] and computational [10] observations of the Cu self-roughening, although it is not yet clear whether the exact mechanism of roughening is captured correctly by our model.

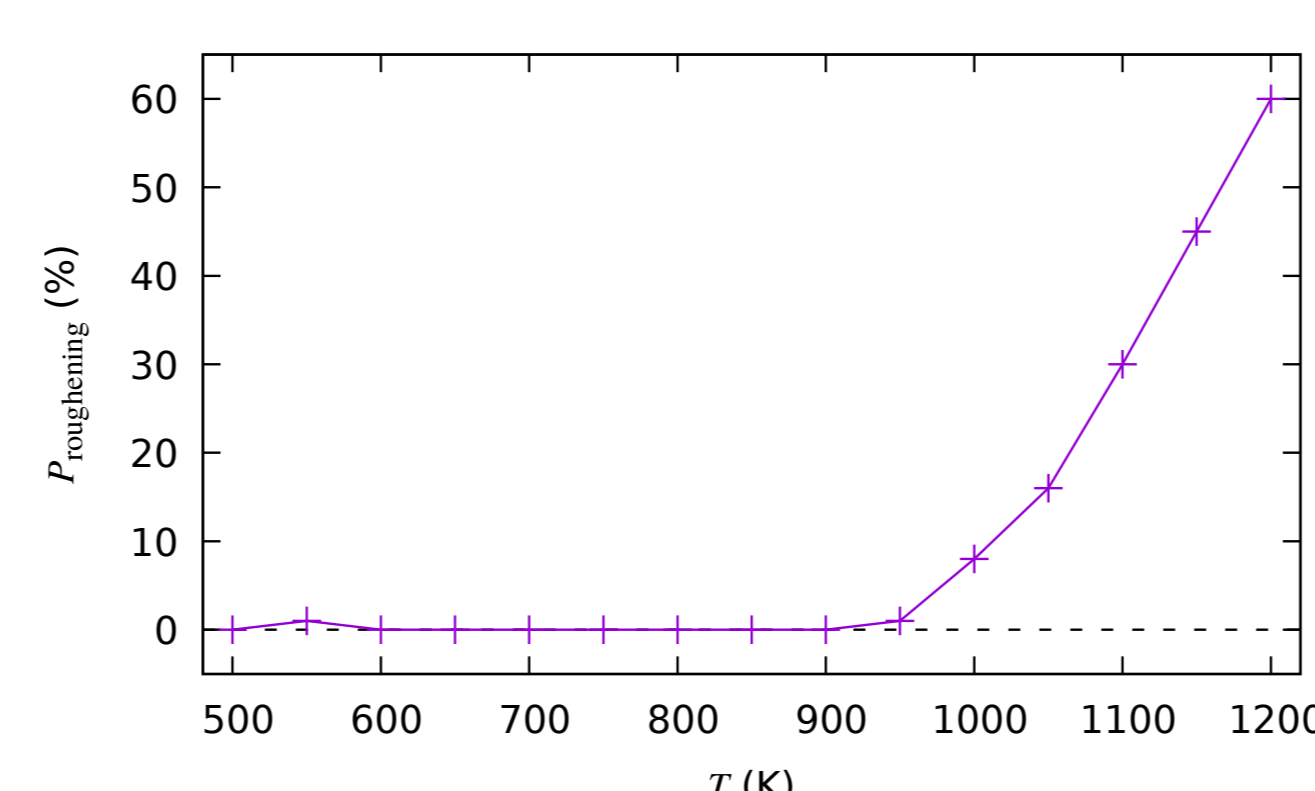


Figure 7: Probability for the roughening to occur before the tip flattens, as a function of temperature.

The results of the nanoparticle relaxations at 900 K are shown in fig. 8. All initial shapes tended towards the minimal energy configuration, i.e. the Wulff construction. This gives further confidence that the model correctly describes the thermodynamic properties of the Cu system.

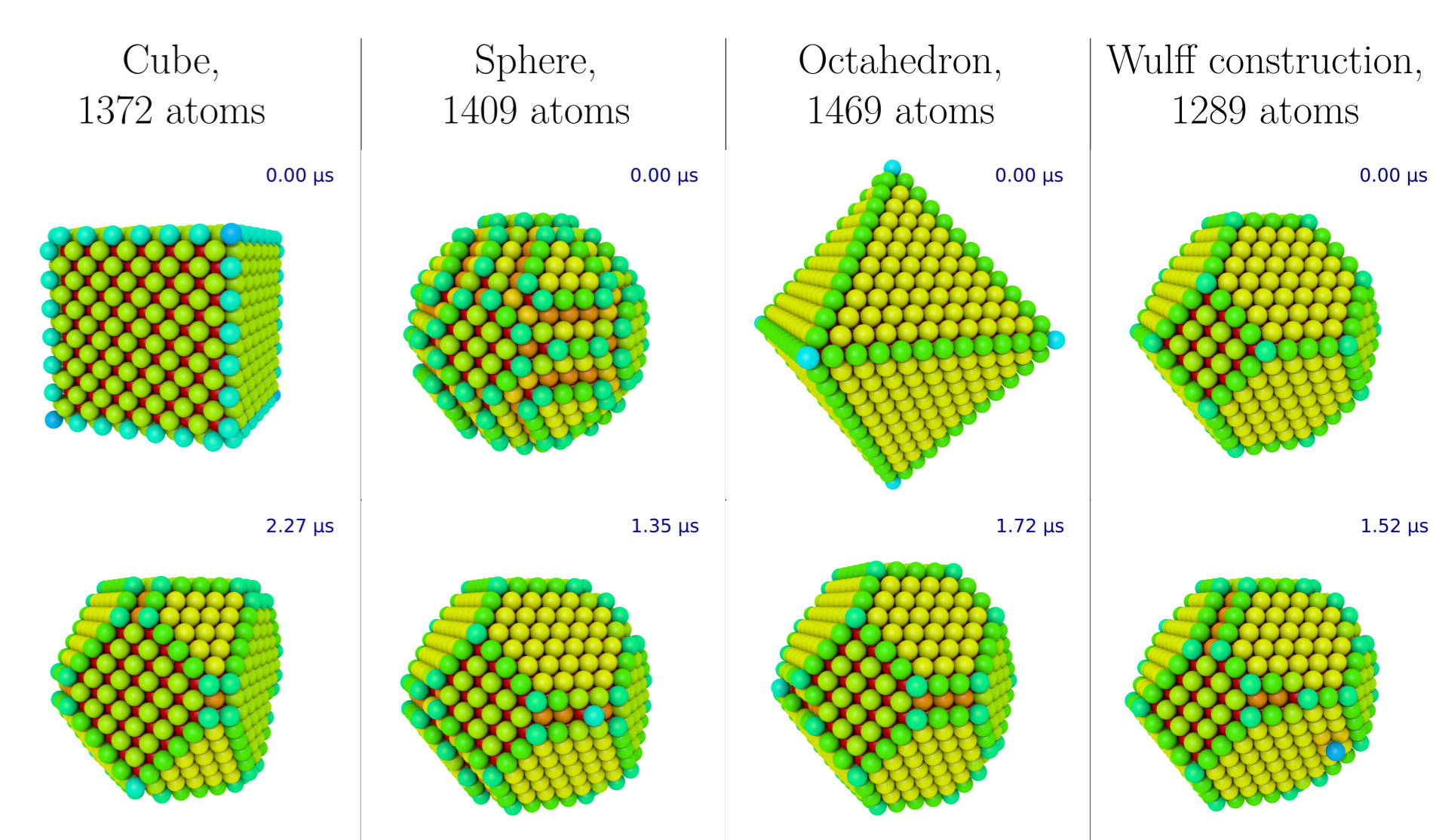


Figure 8: Relaxation of nanoparticles of different initial shapes at 900 K.

Snapshots of the single and crossing nanowires are shown in fig. 9. The wires were observed to break into splinters by diffusion starting at 1000 K, with the systems of crossing wires breaking much earlier than the single wires, and always first at the junction of two wires. This is consistent with what was observed for Au nanowires in ref. [11]. The mean time for the single wires to break was 260 ± 30 ns; the crossing wires had the first breaking occur at 8.3 ± 0.8 ns, and complete breaking at all four points around the junction at 23.1 ± 1.4 ns.

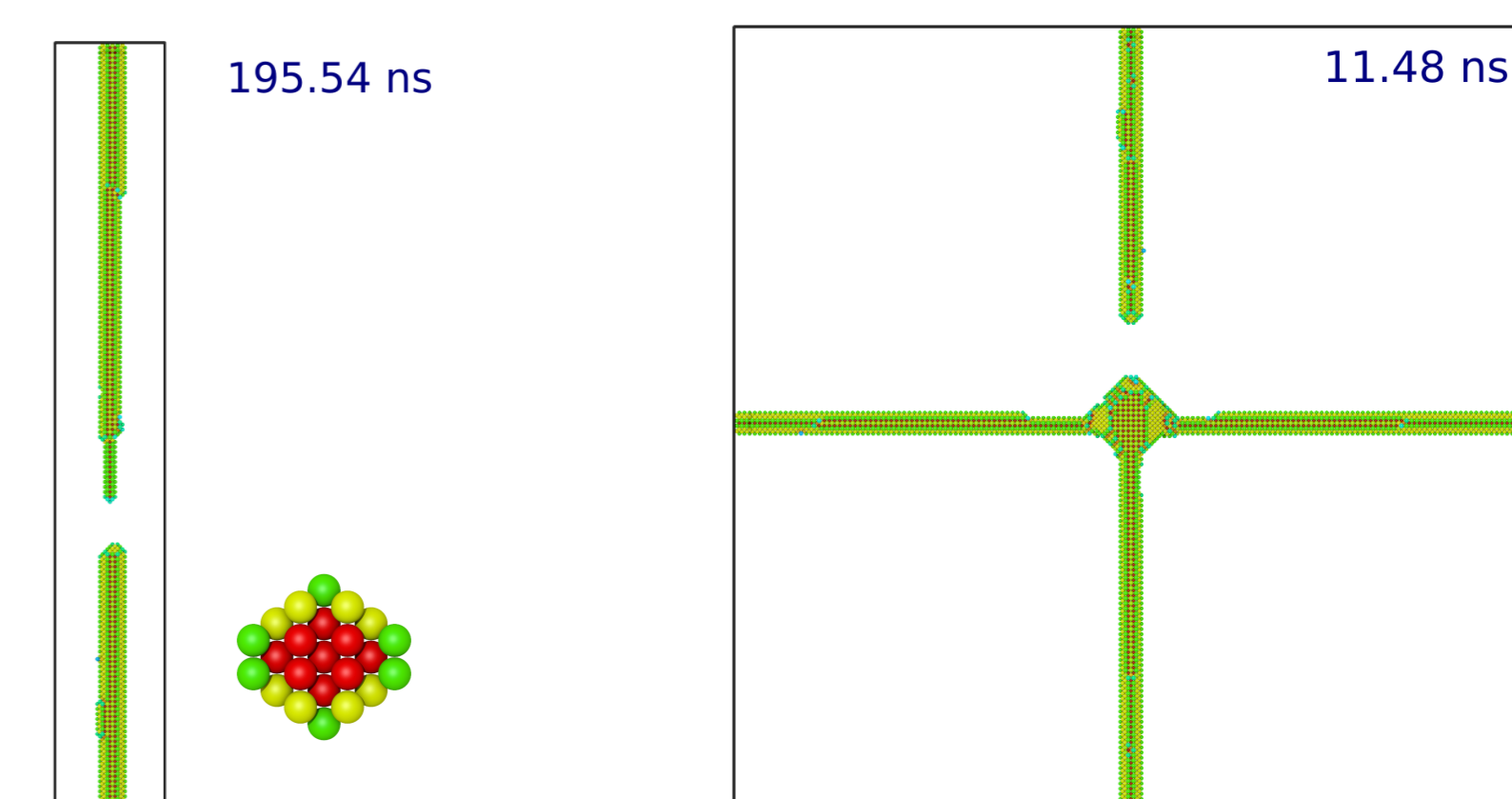


Figure 9: Snapshots of a single $\{110\}$ -oriented nanowire (left) and a system of crossing wires (right) at 1000 K, at the moment when the first breaking occurs. The length of the nanowires is 400 nm. Inset is a figure of the cross-section of the nanowire.

CONCLUSIONS

- The machine learning parameterized KMC model performs at equal level with our earlier model for Cu. The model is ready for expansion to multiple elements, or inclusion of the electric field.
- The thermodynamics of the Cu system can be described very accurately, even though the ANN learns the thermodynamic properties only implicitly through the barrier regression training.
- Roughening of the $\{110\}$ surface is observed very near to the known roughening temperature of this surface. Nevertheless we advise caution when using our model at elevated temperatures, since the mechanism of roughening may not be well described.

REFERENCES

- [1] V. Jansson et al. *Nanotechnology* 27.26 (2016), p. 265708.
- [2] E. Baibuz et al. *Computational Materials Science* 146 (C 2018), pp. 287–302.
- [3] G. Mills et al. *Physical review letters* 72.7 (1994), p. 1124.
- [4] G. Mills et al. *Surface Science* 324.2 (1995), pp. 305–337.
- [5] S. Nissen. *Implementation of a Fast Artificial Neural Network Library (fann)*. Tech. rep. Department of Computer Science University of Copenhagen (DIKU), 2003. URL: <http://fann.sf.net>.
- [6] S. Plimpton. *Journal of computational physics* 117.1 (1995), pp. 1–19.
- [7] J. Kimari et al. (in preparation).
- [8] S. Mochrie. *Physical review letters* 59.3 (1987), p. 304.
- [9] P. Zeppenfeld et al. *Physical review letters* 62.1 (1989), p. 63.
- [10] H. Häkkinen et al. *Physical review letters* 70.16 (1993), p. 2451.
- [11] S. Vigonski et al. *Nanotechnology* 29.1 (2017), p. 015704.